Journal of Scientific Computing (2020) 83:47
https://doi.org/10.1007/s10915-020-01239-4

Penalty-Free Any-Order Weak Galerkin FEMs for Elliptic Problems on Quadrilateral Meshes

Jiangguo Liu[1] · **Simon Tavener**[1] · **Zhuoran Wang**[1]

Received: 17 August 2019 / Revised: 18 May 2020 / Accepted: 20 May 2020

Abstract

This paper presents a family of weak Galerkin finite element methods for elliptic boundary value problems on convex quadrilateral meshes. These new methods use degree $k \geq 0$ polynomials separately in element interiors and on edges for approximating the primal variable. The discrete weak gradients of these shape functions are established in the local Arbogast–Correa AC_k spaces. These discrete weak gradients are then used to approximate the classical gradient in the variational formulation. These new methods do not use any nonphysical penalty factor but produce optimal-order approximation to the primal variable, flux, normal flux, and divergence of flux. Moreover, these new solvers are locally conservative and offer continuous normal fluxes. Numerical experiments are presented to demonstrate the accuracy of this family of new methods.

Keywords Arbogast–Correa spaces · Elliptic boundary value problems · Penalty-free · Quadrilateral meshes · Weak Galerkin

Mathematics Subject Classification 65N15 · 65N30 · 76S06

J. Liu and Z. Wang were partially supported by US NSF under Grant DMS-1819252. S. Tavener was partially supported by US NSF under Grant DMS-1720473.

✉ Jiangguo Liu
liu@math.colostate.edu

Simon Tavener
tavener@math.colostate.edu

Zhuoran Wang
wangz@math.colostate.edu

1 Department of Mathematics, Colorado State University, Fort Collins, CO 80523-1874, USA

Published online: 01 June 2020

1 Introduction

This paper concerns finite element methods for 2-dim elliptic boundary value problems prototyped as

$$\begin{cases} \nabla \cdot (-\mathbf{K}\nabla p) \equiv \nabla \cdot \mathbf{u} = f, & \mathbf{x} \in \Omega, \\ p = p_D, & \mathbf{x} \in \Gamma^D, \\ \mathbf{u} \cdot \mathbf{n} = u_N, & \mathbf{x} \in \Gamma^N, \end{cases} \tag{1}$$

where Ω is a polygonal domain, p is the unknown primal variable, $\mathbf{K}$ a 2×2 coefficient matrix that is uniformly symmetric positive-definite (SPD), f a known function, p_D, u_N Dirichlet and Neumann boundary data, respectively, $\mathbf{n}$ the outward unit normal vector on $\partial\Omega$ that has a nonoverlapping decomposition $\Gamma^D \cup \Gamma^N$.

The above elliptic problems arise from many real-world applications, for example, flow in porous media and heat or electrical conduction in composite materials. For ease of presentation, we adopt the terminology for flow in porous media to interpret p as the pressure in a single-phase steady flow, $\mathbf{K}$ as the conductivity matrix (the ratio of permeability and fluid viscosity), $\mathbf{u} = -\mathbf{K}\nabla p$ as the Darcy velocity, and f as a source term. Accordingly, $\mathbf{u} \cdot \mathbf{n}$ is the normal flux on any edge in a given mesh, and $\nabla \cdot \mathbf{u}$ is the divergence (div) of the velocity.

For development of finite element methods for the elliptic problems in (1), here are some main considerations:

(i) Preserving physical properties: Local conservation, flux normal continuity;
(ii) Optimal-order accuracy in pressure, velocity, normal flux, and divergence of velocity;
(iii) Easy implementation: SPD discrete linear systems.

For the continuous Galerkin (CG) FEMs in their original forms, it is well known that they are not locally conservative and do not offer continuous normal fluxes. Postprocsing [8] or enrichment by elementwise constants [23] renders CG FEMs these two important physical properties. The discontinuous Galerkin (DG) FEMs are locally conservative by design. Hybridization [12] provides continuous normal fluxes and reduces global degrees of freedom to those on interelement boundaries. The mixed finite element methods (MFEMs) by design are locally conservative and produce continuous normal fluxes. But the original forms of MFEMs result in indefinite linear systems. Hybridization [6] converts such an indefinite linear system into an SPD system that involves the flux unknowns, primal unknowns, and Lagrange multipliers. Schur complement [1] or static condensation [10] can further reduce the size of the discrete linear system and simplified it into an SPD system.

The hybridizable discontinuous Galerkin (HDG) FEMs form another large class, in addition to the classical mixed FEMs. It is not a surprise to see the connection and interaction among these three classes of FEMs, especially, the similarities and differences between WG and HDG finite element methods. In seeking approximate solutions to PDEs based on finite elements, both HDG and WG consider quantities or variables in element interiors and on mesh skeleton. These quantities could be primal variables, dual variables or fluxes, normal traces, and multipliers. The HDG methodology, as of our understanding, relies mainly on hybridization, see [10–13] and references therein. HDG FEMs are based on deep analysis of the relationships among approximation subspaces for those quantities, which produce a variety of choices for devising finite elements.

The WG methodology [25] relies mainly on integration by parts for reconstruction of differential operators in the weak sense at the element level. Generally speaking, approximants to the primal variable are defined separately in element interiors and on inter-element boundaries and then used to construct discrete weak gradients, curls, or divergences, which are then used to approximate the classical differential operators in the variational forms. But these discrete weak gradients do not constitute degrees of freedom. WG finite element methods have been developed for a wide range of problems, e.g., elliptic problems [20,21], Darcy flow [17,19], elasticity [15,24,29], two-phase flow problems [14], Stokes flow [22], and coupled Stokes–Darcy flow [9].

In this paper, we develop a family of any-order penalty-free weak Galerkin FEMs for elliptic problems on general convex quadrilateral meshes. Compared to triangular meshes, quadrilateral meshes can also accommodate complicated domain geometry while involving less unknowns.

These new WG methods use degree $k \geq 0$ polynomials inside elements and on interelement boundaries separately for approximating the primal variable. The discrete weak gradients of these shape functions are established in the elementwise Arbogast–Correa AC_k spaces [1]. These discrete weak gradients are then used to approximate the classical gradient in the variational formulation for the elliptic problems (1). These new WG methods do not involve any nonphysical penalization but produce optimal-order approximation to the primal variable, flux, normal flux, and divergence of flux. Moreover, these new solvers are locally conservative and offer continuous normal fluxes. The resulting discrete linear systems are symmetric positive-definite.

The rest of this paper is organized as follows. Section 2 briefly discusses the Arbogast–Correa spaces $AC_k(k \geq 0)$. Section 3 discusses construction of weak Galerkin elements $(P_k, P_k; AC_k)$. Section 4 develops a family of numerical schemes using these new WG finite elements to solve the elliptic problems (1) on convex quadrilateral meshes. Section 5 presents rigorous error analysis for these new WG FEMs. Section 6 briefly discusses implementation strategies and then presents numerical experiments to illustrate the theoretical results. Section 7 concludes the paper with some remarks.

2 Local and Global Arbogast–Correa Spaces $AC_k(k \geq 0)$

Compared to the classical Raviart–Thomas elements [7] or the Arnold–Boffi–Falk elements [5], the Arbogast–Correa elements constructed recently in [1] for convex quadrilaterals have better approximation properties and less degrees of freedom. The $AC_k(k \geq 0)$ spaces are constructed using both unmapped vector-valued polynomials and rational functions obtained via the Piola transformation.

Let E be a convex quadrilateral and $k \geq 0$ be an integer. The local Arbogast–Correa space on E is defined as

$$AC_k(E) = P_k^2(E) + \mathbf{x}\widetilde{P}_k(E) + \mathbb{S}_k(E), \tag{2}$$

where $P_k^2(E)$ is the space of bivariate vector-valued polynomials defined on E with total degree at most k, $\widetilde{P}_k(E)$ is the space of bivariate homogeneous scalar-valued polynomials with degree exactly k, and $\mathbb{S}_k(E)$ is a supplementary space of vector-valued rational functions obtained via the Piola transformation.

Clearly,

$$\dim(P_k^2) = (k+1)(k+2), \qquad \dim(\widetilde{P}_k) = k+1.$$

However,

$$\dim(\mathbb{S}_k) = 1 \text{ if } k = 0, \qquad \dim(\mathbb{S}_k) = 2 \text{ if } k > 0.$$

If we set $s_k = \dim(\mathbb{S}_k)$, then

$$\dim(AC_k(E)) = (k+1)(k+3) + s_k. \tag{3}$$

Note that $(k+1)(k+3) = \dim(RT_k)$, i.e., the dimension of the k-th order Raviart–Thomas (RT) space on a triangle [7]. So s_k is the additional degrees of freedom needed for augmenting the RT space on a quadrilateral [1].

For convenience, we write $\mathbb{S}_k = \mathcal{P}_E \hat{\mathbb{S}}_k$, where $\mathcal{P}_E$ is the Piola transformation. Let $(\hat{x}, \hat{y})$ be the coordinates in the reference element $[0, 1]^2$. According to [1], for $k = 0$,

$$\hat{\mathbb{S}}_0 = \text{Span}\{\mathbf{curl}(\hat{x}\hat{y})\}. \tag{4}$$

For $k \geq 1$,

$$\hat{\mathbb{S}}_k = \text{Span}\{\mathbf{curl}((1-\hat{x}^2)\hat{x}^{k-1}\hat{y}),\ \mathbf{curl}(\hat{x}^{k-1}\hat{y}(1-\hat{y}^2))\}. \tag{5}$$

Roughly speaking, $P_k^2(E)$ takes care of approximation for a vector field on a convex quadrilateral, $\mathbf{x}\widetilde{P}_k(E)$ takes care of approximation in its divergence, whereas $\mathbb{S}_k$ offers a divergence-free supplement.

When the Arbogast–Correa elements are used in the mixed finite element setting [1] for solving elliptic problems, global basis functions (especially those on the common edges) need to be carefully constructed, to ensure that the velocity is being approximated from the global AC_k space on the whole mesh, which is a finite-dimensional subspace of $H(\text{div}, \Omega)$.

However, when the WG methods in this paper are applied to elliptic problems, only the local basis functions for the AC_k spaces on individual quadrilaterals are needed. We will show later in Sect. 4 that the velocity obtained from the weak Galerkin methods $(P_k, P_k; AC_k)$ is automatically in the global AC_k space and hence in $H(\text{div}, \Omega)$.

3 WG $(P_k, P_k; AC_k)(k \geq 0)$ Finite Elements on Quadrilaterals

Weak Galerkin finite elements use separate basis functions in element interiors and on interelement boundaries. These basis functions are different than those basis functions used in the continuous or discontinuous Galerkin methods. We call them discrete weak functions.

Let $k \geq 0$ be an integer and E be a convex quadrilateral. Let $P_k(E^\circ)$ be the space of polynomials defined in E° with degree at most k, and similarly, $P_k(E^\partial)$ be the space of piecewise polynomials defined on E^∂ with degree at most k. Let $AC_k(E)$ be the space of vector-valued polynomials/rationals discussed in the previous section.

Let $\phi = \{\phi^\circ, \phi^\partial\}$ be a discrete weak function such that $\phi^\circ \in P_k(E^\circ)$ and $\phi^\partial \in P_k(E^\partial)$. Note that ϕ° is defined for the element interior only, whereas ϕ^∂ is defined on the element boundary only. We define $\nabla_w \phi \in AC_k(E)$ by

$$\int_E (\nabla_w \phi) \cdot \mathbf{w} = \int_{E^\partial} \phi^\partial (\mathbf{w} \cdot \mathbf{n}) - \int_{E^\circ} \phi^\circ (\nabla \cdot \mathbf{w}) \qquad \forall \mathbf{w} \in AC_k(E), \tag{6}$$

or in slightly different notations,

$$(\nabla_w \phi, \mathbf{w})_E = \langle \phi^\partial, \mathbf{w} \cdot \mathbf{n} \rangle_{E^\partial} - (\phi^\circ, \nabla \cdot \mathbf{w})_{E^\circ}. \tag{7}$$

For any such discrete weak function ϕ, we need to solve a small-size SPD linear system (7) to find the linear combination coefficients for $\nabla_w \phi$ in the local basis functions of $AC_k(E)$.

As shown in the next section, the above discrete weak gradients will be used to approximate the classical gradient in the variational form for elliptic problems.

4 WG Schemes for Elliptic Problems on Quadrilateral Meshes

Let Ω be a polygonal domain equipped with a shape-regular convex quadrilateral mesh $\mathcal{E}_h$ [26]. Let Γ_h^D be the set of all edges on the Dirichlet boundary Γ^D and Γ_h^N be the set of all edges on the Neumann boundary Γ^N. Let S_h be the space of discrete weak functions on $\mathcal{E}_h$ that are degree k polynomials separately in element interiors and on edges, and S_h^0 be the subspace of functions in S_h that vanish on Γ_h^D.

To proceed, we define *an* L^2*-projection* $Q_h = \{Q_h^\circ, Q_h^\partial\}$ such that for any quadrilateral element $E \in \mathcal{E}_h$, Q_h° is a local L^2-projection that maps $L^2(E^\circ)$ functions into the space of degree k polynomials in E°, and in the same spirit, Q_h^∂ maps $L^2(E^\partial)$ functions into the space of piecewise degree k polynomials on E^∂. We also define a local L^2-projection $\mathbf{Q}_h$ that maps $L^2(E)^2$ to $AC_k(E)$.

WG scheme for pressure on a quadrilateral mesh. Seek $p_h = \{p_h^\circ, p_h^\partial\} \in S_h$ such that $p_h^\partial|_{\Gamma_h^D} = Q_h^\partial(p_D)$ and

$$\mathcal{A}_h(p_h, q) = \mathcal{F}_h(q), \qquad \forall q = \{q^\circ, q^\partial\} \in S_h^0, \tag{8}$$

where

$$\mathcal{A}_h(p_h, q) = \sum_{E \in \mathcal{E}_h} \int_E \mathbf{K}\nabla_w p_h \cdot \nabla_w q \tag{9}$$

and

$$\mathcal{F}_h(q) = \sum_{E \in \mathcal{E}_h} \int_{E^\circ} f\, q^\circ - \sum_{e \in \Gamma_h^N} \int_e u_N q^\partial. \tag{10}$$

After the numerical pressure p_h is solved from (8), an elementwise **numerical velocity** is obtained by performing a local L^2-projection back into the local subspace AC_k:

$$\mathbf{u}_h = \mathbf{Q}_h(-\mathbf{K}\nabla_w p_h). \tag{11}$$

But this projection is not needed when $\mathbf{K}$ is an elementwise constant scalar matrix. Then the **bulk normal flux** on an edge e is defined as

$$\int_{e \subset E^\partial} \mathbf{u}_h \cdot \mathbf{n}_e. \tag{12}$$

Regardless of mesh quality, these new WG finite element methods possess two important properties: *local mass conservation* and *normal flux continuity*.

Theorem 1 (Local mass conservation) *Let $E \in \mathcal{E}_h$ be a quadrilateral. There holds*

$$\int_E f = \int_{E^\partial} \mathbf{u}_h \cdot \mathbf{n}. \tag{13}$$

Proof In the finite element scheme (8), we take a test function q so that $q|_{E^\circ} = 1$ but it vanishes on all edges and inside all other elements. Then

$$\begin{aligned}\int_E f &= \int_E (\mathbf{K}\nabla_w p_h) \cdot \nabla_w q = \int_E \mathbf{Q}_h(\mathbf{K}\nabla_w p_h) \cdot \nabla_w q = -\int_E \mathbf{u}_h \cdot \nabla_w q \\ &= -\int_{E^\partial} q^\partial (\mathbf{u}_h \cdot \mathbf{n}) + \int_{E^\circ} q^\circ (\nabla \cdot \mathbf{u}_h) = \int_{E^\circ} \nabla \cdot \mathbf{u}_h = \int_{E^\partial} \mathbf{u}_h \cdot \mathbf{n}.\end{aligned}$$

It is interesting to note that

- The 1st "=" comes from the WG finite element scheme;

- The 2nd "=" uses the definition of projection $\mathbf{Q}_h$;
- The 3rd "=" uses the definition of numerical velocity;
- The 4th "=" uses the definition of discrete weak gradient;
- The 5th "=" uses the definition of this particular test function q;
- The 6th "=" uses Gauss Divergence Theorem on a function in AC_k.

□

Theorem 2 (Continuity of bulk normal flux) *Let e be an edge shared by two convex quadrilaterals E_1, E_2 and $\mathbf{n}_1, \mathbf{n}_2$ be the outward unit normal vectors on e respectively for E_1, E_2. There holds*

$$\int_e \mathbf{u}_h^{(1)} \cdot \mathbf{n}_1 + \int_e \mathbf{u}_h^{(2)} \cdot \mathbf{n}_2 = 0, \tag{14}$$

where $\mathbf{u}_h^{(j)} = \mathbf{u}_h|_{E_j}$ for $j = 1, 2$.

Proof In the FE scheme (8), we take a test function $q = \{q^\circ, q^\partial\}$ so that

- $q^\partial = 1$ only on edge e but $= 0$ on all other edges;
- $q^\circ = 0$ in the interior of any quadrilateral element.

The definitions of $\mathbf{Q}_h$ and discrete weak gradient together with Gauss Divergence Theorem imply that

$$\begin{aligned}
0 &= \int_{E_1} (\mathbf{K}\nabla_w p_h) \cdot \nabla_w q + \int_{E_2} (\mathbf{K}\nabla_w p_h) \cdot \nabla_w q \\
&= \int_{E_1} \mathbf{Q}_h(\mathbf{K}\nabla_w p_h) \cdot \nabla_w q + \int_{E_2} \mathbf{Q}_h(\mathbf{K}\nabla_w p_h) \cdot \nabla_w q \\
&= \int_{E_1} (-\mathbf{u}_h^{(1)}) \cdot \nabla_w q + \int_{E_2} (-\mathbf{u}_h^{(2)}) \cdot \nabla_w q \\
&= -\int_e \mathbf{u}_h^{(1)} \cdot \mathbf{n}_1 q^\partial + \int_{E_1^\circ} (\nabla \cdot \mathbf{u}_h^{(1)}) q^\circ - \int_e \mathbf{u}_h^{(2)} \cdot \mathbf{n}_2 q^\partial + \int_{E_2^\circ} (\nabla \cdot \mathbf{u}_h^{(2)}) q^\circ \\
&= -\int_e \mathbf{u}_h^{(1)} \cdot \mathbf{n}_1 - \int_e \mathbf{u}_h^{(2)} \cdot \mathbf{n}_2,
\end{aligned}$$

which yields the desired result in the above theorem. □

Remark 1 A re-examination of the above proof yields

$$\int_e \mathbf{u}_h^{(1)} \cdot \mathbf{n}_1 q^\partial + \int_e \mathbf{u}_h^{(2)} \cdot \mathbf{n}_2 q^\partial = 0 \qquad \forall q^\partial \in P_k(e), \tag{15}$$

which implies that $\mathbf{u}_h \in H(\mathrm{div}, \Omega)$. This is related to (20) also.

Errors in pressure, velocity, and normal flux are measured in the following norms:

$$\|p - p_h^\circ\|^2 = \sum_{E \in \mathcal{E}_h} \|p - p_h^\circ\|^2_{L^2(E^\circ)}, \tag{16}$$

$$\|\mathbf{u} - \mathbf{u}_h\|^2 = \sum_{E \in \mathcal{E}_h} \|\mathbf{u} - \mathbf{u}_h\|^2_{L^2(E)^2}, \tag{17}$$

$$\|(\mathbf{u} - \mathbf{u}_h) \cdot \mathbf{n}\|^2_{\mathcal{F}_h} = \sum_{E \in \mathcal{E}_h} \sum_{e \subset E^\partial} \frac{|E|}{|e|} \|\mathbf{u} \cdot \mathbf{n} - \mathbf{u}_h \cdot \mathbf{n}\|^2_{L^2(e)}, \tag{18}$$

where $\mathcal{F}_h$ denotes the set of all edges, namely, the skeleton of a given mesh $\mathcal{E}_h$. This helps us distinguish the norm for errors in normal flux from the other norms for quantities in elements. Here the norm for errors in normal flux is adopted from [27], which "gives an appropriate scaling of size of $|\Omega|$ for a unit vector".

Under the assumptions that quadrilaterals meshes are shape-regular or quasi-uniform, and the exact solution and the coefficient matrix $\mathbf{K}$ are sufficiently smooth, we can show that the accuracy in the primal variable, flux, normal flux, and divergence of flux are in the form

$$\|p - p_h^\circ\| = \mathcal{O}(h^{k+1}), \qquad \|\mathbf{u} - \mathbf{u}_h\| = \mathcal{O}(h^{k+1}),$$
$$\|\mathbf{u}\cdot\mathbf{n} - \mathbf{u}_h\cdot\mathbf{n}\|_{\mathcal{F}_h} = \mathcal{O}(h^{k+1}), \qquad \|\nabla\cdot\mathbf{u} - \nabla\cdot\mathbf{u}_h\| = \mathcal{O}(h^{k+1}).$$

These results will be stated and proved rigorously in the next section.

5 Analysis

This section presents rigorous error analysis for the WG FEMs developed in the previous section. For convenience, we use $A \lesssim B$ to denote an inequality $A \le CB$, in which C is an absolute constant that is independent of the mesh size h but may take different values in different appearances. Similarly, $A \approx B$ means both $A \lesssim B$ and $B \lesssim A$.

Similar to [19,25], the analysis relies on approximation properties of two operators that map from spaces of vector-valued functions to the local or global AC_k spaces. The first one is the local L^2-projection operator $\mathbf{Q}_h$ introduced at the beginning of Sect. 4. The second one is the global interpolation operator defined below (assuming $\epsilon > 0$):

$$\Pi_h : H(\mathrm{div}, \Omega) \cap L^{2+\epsilon}(\Omega)^2 \longrightarrow AC_k(\mathcal{E}_h), \tag{19}$$

which is actually a gluing-together of the local interpolation operators Π_E defined in [1]. On each $E \in \mathcal{E}_h$, we have $(\Pi_h\mathbf{v})|_E = \Pi_E\mathbf{v}$. Note that the global $AC_k(\mathcal{E}_h)$ space is a subspace of $H(\mathrm{div}, \Omega)$.

Let E be a convex quadrilateral and e be any of its edge. It is known [1] that for any $\mathbf{v} \in AC_k(E)$,

$$\nabla\cdot\mathbf{v} \in P_k(E), \qquad \mathbf{v}\cdot\mathbf{n} \in P_k(e). \tag{20}$$

It is also known from [1] that the following approximation properties hold.

$$\|\mathbf{v} - \mathbf{Q}_h\mathbf{v}\|_{L^2(E)^2} \lesssim h_E^j\|\mathbf{v}\|_{H^j(E)^2}, \qquad j = 0, 1, \ldots, k+1, \tag{21}$$
$$\|\mathbf{v} - \Pi_h\mathbf{v}\|_{L^2(E)^2} \lesssim h_E^j\|\mathbf{v}\|_{H^j(E)^2}, \qquad j = 1, \ldots, k+1, \tag{22}$$
$$\|\nabla\cdot(\mathbf{v} - \Pi_h\mathbf{v})\|_{L^2(E)} \lesssim h_E^j\|\nabla\cdot\mathbf{v}\|_{H^j(E)}, \qquad j = 0, 1, \ldots, k+1. \tag{23}$$

Furthermore, Π_h satisfies the commuting property

$$Q_h^\circ(\nabla\cdot\mathbf{v}) = \nabla\cdot(\Pi_h\mathbf{v}).$$

In other words, for any $\mathbf{v} \in H(\mathrm{div}, \Omega) \cap L^{2+\epsilon}(\Omega)^2$, there holds [1]

$$(\nabla\cdot\mathbf{v}, \phi^\circ)_{E^\circ} = (\nabla\cdot(\Pi_h\mathbf{v}), \phi^\circ)_{E^\circ} \qquad \forall\phi^\circ \in P_k(E^\circ) \quad \forall E \in \mathcal{E}_h. \tag{24}$$

Lemma 1 *For any $E \in \mathcal{E}_h$ and any $p \in H^1(E)$, there holds*

$$\nabla_w(Q_h p) = \mathbf{Q}_h(\nabla p). \tag{25}$$

Proof For any $\mathbf{v} \in AC_k(E)$, by the definitions of discrete weak gradient (7) and Q_h, and integration by parts, we have

$$\begin{aligned}(\nabla_w(Q_h p), \mathbf{v})_E &= -(Q_h^\circ p, \nabla \cdot \mathbf{v})_{E^\circ} + \langle Q_h^\partial p, \mathbf{v} \cdot \mathbf{n}\rangle_{E^\partial} \\ &= -(p, \nabla \cdot \mathbf{v})_E + \langle p, \mathbf{v} \cdot \mathbf{n}\rangle_{E^\partial} \\ &= (\nabla p, \mathbf{v})_E = (\mathbf{Q}_h(\nabla p), \mathbf{v})_E,\end{aligned}$$

which proves (25). □

We continue to establish lemmas that are useful for error estimation.

Lemma 2 *For any $\mathbf{v} \in H(div, \Omega) \cap L^{2+\epsilon}(\Omega)^2$ and any $\phi = \{\phi^\circ, \phi^\partial\} \in S_h^0$, there holds*

$$\sum_{E \in \mathcal{E}_h} (\nabla \cdot \mathbf{v}, \phi^\circ)_{E^\circ} = -\sum_{E \in \mathcal{E}_h} (\Pi_h \mathbf{v}, \nabla_w \phi)_E + \sum_{e \in \Gamma_h^N} \langle \Pi_h \mathbf{v} \cdot \mathbf{n}, \phi^\partial\rangle_e. \tag{26}$$

Proof By (24), the definitions of discrete weak gradient (7) and Π_h, we have

$$\begin{aligned}\sum_{E \in \mathcal{E}_h} (\nabla \cdot \mathbf{v}, \phi^\circ)_{E^\circ} &= \sum_{E \in \mathcal{E}_h} (\nabla \cdot (\Pi_h \mathbf{v}), \phi^\circ)_{E^\circ} \\ &= -\sum_{E \in \mathcal{E}_h} (\Pi_h \mathbf{v}, \nabla_w \phi)_E + \sum_{E \in \mathcal{E}_h} \langle \Pi_h \mathbf{v} \cdot \mathbf{n}, \phi^\partial\rangle_{E^\partial} \\ &= -\sum_{E \in \mathcal{E}_h} (\Pi_h \mathbf{v}, \nabla_w \phi)_E + \sum_{e \in \Gamma_h^N} \langle \Pi_h \mathbf{v} \cdot \mathbf{n}, \phi^\partial\rangle_e,\end{aligned}$$

which proves (26). □

Lemma 3 *Assume that $p \in H^{k+1}(\Omega)$ and $\mathbf{u} \in H(div, \Omega) \cap L^{2+\epsilon}(\Omega)^2 \cap H^k(\Omega)^2$ for an integer $k \geq 0$. There holds*

$$\|\nabla_w(p_h - Q_h p)\| \lesssim h^k. \tag{27}$$

Proof Let $\phi = \{\phi^\circ, \phi^\partial\} \in S_h^0$ be arbitrary. By (1) and Lemma 2, we have

$$\begin{aligned}\sum_{E \in \mathcal{E}_h} (f, \phi^\circ)_{E^\circ} &= \sum_{E \in \mathcal{E}_h} (\nabla \cdot (-\mathbf{K}\nabla p), \phi^\circ)_{E^\circ} \\ &= \sum_{E \in \mathcal{E}_h} (\Pi_h(\mathbf{K}\nabla p), \nabla_w \phi)_E - \sum_{e \in \gamma_h^N} \langle \Pi_h(\mathbf{K}\nabla p) \cdot \mathbf{n}, \phi^\partial\rangle_e. \end{aligned}\tag{28}$$

Combining this with (8) and the definition of Π_h, we obtain

$$\begin{aligned}\mathcal{A}_h(p_h, \phi) &= \sum_{E \in \mathcal{E}_h} (\Pi_h(\mathbf{K}\nabla p), \nabla_w \phi)_E - \sum_{e \in \Gamma_h^N} \langle (\mathbf{u} - \Pi_h \mathbf{u}) \cdot \mathbf{n}, \phi^\partial\rangle_e \\ &= \sum_{E \in \mathcal{E}_h} (\Pi_h(\mathbf{K}\nabla p), \nabla_w \phi)_E. \end{aligned}\tag{29}$$

According to Lemma 1, we have

$$\mathcal{A}_h(Q_h p, \phi) = \sum_{E \in \mathcal{E}_h} (\mathbf{K}\nabla_w(Q_h p), \nabla_w \phi)_E = \sum_{E \in \mathcal{E}_h} (\mathbf{K}\mathbf{Q}_h(\nabla p), \nabla_w \phi)_E. \tag{30}$$

Subtracting (30) from (29), we obtain the following error equation:

$$\mathcal{A}_h(p_h - Q_h p, \phi) = \sum_{E\in\mathcal{E}_h} (\Pi_h(\mathbf{K}\nabla p) - \mathbf{K}\mathbf{Q}_h(\nabla p), \nabla_w \phi)_E \qquad \forall \phi \in S_h^0. \tag{31}$$

Denoting $e_h = p_h - Q_h p \in S_h^0$ and taking $\phi = e_h$ in (31), we obtain

$$\begin{aligned} \mathcal{A}_h(e_h, e_h) &= \textstyle\sum_{E\in\mathcal{E}_h} (\Pi_h(\mathbf{K}\nabla p) - \mathbf{K}\nabla p, \nabla_w e_h)_E \\ &\quad + \textstyle\sum_{E\in\mathcal{E}_h} (\mathbf{K}\nabla p - \mathbf{K}\mathbf{Q}_h(\nabla p), \nabla_w e_h)_E. \end{aligned} \tag{32}$$

The 1st term on the right-hand side of (32) can be estimated as follows [by applying (22)]

$$\begin{aligned} \sum_{E\in\mathcal{E}_h} (\Pi_h(\mathbf{K}\nabla p) - \mathbf{K}\nabla p, \nabla_w e_h)_E &\le \sum_{E\in\mathcal{E}_h} \|\Pi_h(\mathbf{K}\nabla p) - \mathbf{K}\nabla p\|_{L^2(E)^2} \|\nabla_w e_h\|_{L^2(E)^2} \\ &\le \sum_{E\in\mathcal{E}_h} h_E^k \|\mathbf{u}\|_{H^k(E)^2} \|\nabla_w e_h\|_{L^2(E)^2} \\ &\lesssim h^k \|\nabla_w e_h\|. \end{aligned} \tag{33}$$

Similarly, the 2nd term on the right-hand side of (32) can be estimated as [by applying (21)]

$$\begin{aligned} \sum_{E\in\mathcal{E}_h} (\mathbf{K}\nabla p - \mathbf{K}\mathbf{Q}_h(\nabla p), \nabla_w e_h)_E &\lesssim \sum_{E\in\mathcal{E}_h} \|\nabla p - \mathbf{Q}_h(\nabla p)\|_{L^2(E)^2} \|\nabla_w e_h\|_{L^2(E)^2} \\ &\lesssim \sum_{E\in\mathcal{E}_h} h_E^k \|p\|_{H^{k+1}(E)} \|\nabla_w e_h\|_{L^2(E)^2} \\ &\lesssim h^k \|\nabla_w e_h\|. \end{aligned} \tag{34}$$

Finally, by combining (32)–(34), we arrive at

$$\|\nabla_w e_h\|^2 \lesssim \mathcal{A}_h(e_h, e_h) \lesssim h^k \|\nabla_w e_h\|,$$

which yields the estimate (27) in Lemma 3. □

Remark 2 Based on the techniques used in the proof of Lemma 3 [see (33)–(34)], we can further show that

$$\|\nabla_w(p_h - Q_h p)\| \lesssim h^{k+1}, \tag{35}$$

provided that $p \in H^{k+2}(\Omega)$ and $\mathbf{u} \in H^{k+1}(\Omega)^2$.

Corollary 1 *Under the assumption of Lemma 3, there holds*

$$\|\nabla p - \nabla_w p_h\| \lesssim h^k. \tag{36}$$

Proof From Lemmas 1, 3, and (21), we have

$$\begin{aligned} \|\nabla p - \nabla_w p_h\| &\le \|\nabla p - \mathbf{Q}_h(\nabla p)\| + \|\mathbf{Q}_h(\nabla p) - \nabla_w p_h\| \\ &= \|\nabla p - \mathbf{Q}_h(\nabla p)\| + \|\nabla_w(Q_h p) - \nabla_w p_h\| \\ &\lesssim h^k, \end{aligned}$$

after applying a triangle inequality. □

Remark 3 Roughly speaking, this corollary reveals that the discrete weak gradient of the numerical pressure is an order k, or "nice", approximation to the classical gradient of the exact pressure.

Theorem 3 (Convergence in velocity) *Assume that* $\mathbf{u} \in H^{k+1}(\Omega)^2$. *There holds*

$$\|\mathbf{u} - \mathbf{u}_h\| \lesssim h^{k+1}. \tag{37}$$

Proof Note that the assumption in Theorem 3 implies that $\nabla p \in H^{k+1}(\Omega)^2$. We have, by Lemma 1, (21), and Remark 2,

$$\begin{aligned}
\|\mathbf{u} - \mathbf{u}_h\| &= \|\mathbf{K}\nabla p - \mathbf{Q}_h(\mathbf{K}\nabla_w p_h)\| \\
&\leq \|\mathbf{K}\nabla p - \mathbf{K}\mathbf{Q}_h(\nabla p)\| + \|\mathbf{K}\mathbf{Q}_h(\nabla p) - \mathbf{Q}_h(\mathbf{K}\nabla_w p_h)\| \\
&= \|\mathbf{K}\nabla p - \mathbf{K}\mathbf{Q}_h(\nabla p)\| + \|\mathbf{K}\mathbf{Q}_h(\nabla p) - \mathbf{K}\mathbf{Q}_h(\nabla_w p_h)\| \\
&\lesssim \|\nabla p - \mathbf{Q}_h(\nabla p)\| + \|\nabla p - \nabla_w p_h\| \\
&\lesssim \|\nabla p - \mathbf{Q}_h(\nabla p)\| + \|\nabla_w(Q_h p - p_h)\| \\
&\lesssim h^{k+1},
\end{aligned}$$

which yields the error estimate in the theorem. □

Theorem 4 (Convergence in bulk normal flux) *Assume* $\mathbf{u} \in H^{k+1}(\Omega)^2$. *There holds*

$$\|(\mathbf{u} - \mathbf{u}_h) \cdot \mathbf{n}\|_{\mathcal{F}_h} \lesssim h^{k+1}. \tag{38}$$

Proof By a triangle inequality, we have

$$\|(\mathbf{u} - \mathbf{u}_h) \cdot \mathbf{n}\|_{\mathcal{F}_h} \leq \|(\mathbf{u} - \Pi_h\mathbf{u}) \cdot \mathbf{n}\|_{\mathcal{F}_h} + \|(\Pi_h\mathbf{u} - \mathbf{u}_h) \cdot \mathbf{n}\|_{\mathcal{F}_h}. \tag{39}$$

Moreover, the mesh $\mathcal{E}_h$ being shape-regular or quasi-uniform implies that $|E|/|e| \lesssim h$ for any convex quadrilateral $E \in \mathcal{E}_h$ and any edge e of E.

Let $\mathbf{w} \in AC_k(E)$ be arbitrary. The first term on the right-hand side of (39) can be estimated by (22), (23), and the trace theorem with scaling:

$$\begin{aligned}
\|(\mathbf{u} - \Pi_h\mathbf{u}) \cdot \mathbf{n}\|^2_{\mathcal{F}_h} &= \sum_{E\in\mathcal{E}_h} \sum_{e\in E^\partial} \frac{|E|}{|e|} \|(\mathbf{u} - \mathbf{w} - \Pi_h(\mathbf{u} - \mathbf{w})) \cdot \mathbf{n}\|^2_{L^2(e)} \\
&\lesssim \sum_{E\in\mathcal{E}_h} \sum_{e\in E^\partial} \frac{|E|}{|e|} \left(h_E^{-1}\|\mathbf{u} - \mathbf{w}\|^2_{L^2(E)^2} + h_E|\mathbf{u} - \mathbf{w}|^2_{H^1(E)^2}\right) \\
&\lesssim h^{2(k+1)},
\end{aligned} \tag{40}$$

where we have also used the following inverse inequality

$$|\mathbf{v}|_{H^1(E)^2} \lesssim h_E^{-1}\|\mathbf{v}\|_{L^2(E)^2} \qquad \forall\, \mathbf{v} \in AC_k(E). \tag{41}$$

This is similar to those stated in [16] Lemma 3.5 and [27] Lemma 3.6.

The second term on the right-hand side of (39) can be bounded by (22), (41), the trace theorem with scaling, and Theorem 3:

$$\begin{aligned}
\|(\Pi_h\mathbf{u} - \mathbf{u}_h) \cdot \mathbf{n}\|^2_{\mathcal{F}_h} &\lesssim \sum_{E\in\mathcal{E}_h} \sum_{e\in E^\partial} \frac{|E|}{|e|} \left(h_E^{-1}\|\Pi_h\mathbf{u} - \mathbf{u}_h\|^2_{L^2(E)^2} + h_E|\Pi_h\mathbf{u} - \mathbf{u}_h|^2_{H^1(E)^2}\right) \\
&\lesssim \|\Pi_h\mathbf{u} - \mathbf{u}_h\|^2 \\
&\lesssim \|\Pi_h\mathbf{u} - \mathbf{u}\|^2 + \|\mathbf{u} - \mathbf{u}_h\|^2 \\
&\lesssim h^{2(k+1)}.
\end{aligned} \tag{42}$$

Finally, the estimate (38) follows from (39), (40), and (42). □

Theorem 5 (Convergence in div of velocity) *Assume $f \in H^{k+1}(\Omega)$. There holds*

$$\|\nabla \cdot \mathbf{u} - \nabla \cdot \mathbf{u}_h\| \lesssim h^{k+1}. \tag{43}$$

Proof Let $\phi = \{\phi^\circ, \phi^\partial\} \in S_h^0$. By (1) and (24), we have

$$\sum_{E \in \mathcal{E}_h} (f, \phi^\circ)_{E^\circ} = \sum_{E \in \mathcal{E}_h} (\nabla \cdot (-\mathbf{K}\nabla p), \phi^\circ)_{E^\circ} = \sum_{E \in \mathcal{E}_h} (\nabla \cdot \mathbf{u}, \phi^\circ)_{E^\circ} = \sum_{E \in \mathcal{E}_h} (\nabla \cdot (\Pi_h \mathbf{u}), \phi^\circ)_{E^\circ}. \tag{44}$$

From (7), (8), and (15), we have

$$\begin{aligned}
\sum_{E \in \mathcal{E}_h} (f, \phi^\circ)_{E^\circ} &= \sum_{E \in \mathcal{E}_h} (\mathbf{K}\nabla_w p_h, \nabla_w \phi)_E \\
&= \sum_{E \in \mathcal{E}_h} (\mathbf{Q}_h(\mathbf{K}\nabla_w p_h), \nabla_w \phi)_E \\
&= \sum_{E \in \mathcal{E}_h} (-\mathbf{u}_h, \nabla_w \phi)_E \\
&= \sum_{E \in \mathcal{E}_h} (\nabla \cdot \mathbf{u}_h, \phi^\circ)_{E^\circ} - \sum_{E \in \mathcal{E}_h} \langle \mathbf{u}_h \cdot \mathbf{n}, \phi^\partial \rangle_{E^\partial} \\
&= \sum_{E \in \mathcal{E}_h} (\nabla \cdot \mathbf{u}_h, \phi^\circ)_{E^\circ}.
\end{aligned} \tag{45}$$

Therefore, we obtain from (44) and (45) that

$$(\nabla \cdot (\Pi_h \mathbf{u} - \mathbf{u}_h), \phi^\circ) = 0. \tag{46}$$

It is clear from (46) that $\nabla \cdot \mathbf{u}_h = \nabla \cdot (\Pi_h \mathbf{u})$, since $\phi^\circ \in P_k(E^\circ)$ is arbitrary. Then (43) follows from (23). □

In order to obtain an L^2-error estimate for the pressure, we consider the following dual problem with a homogeneous Dirichlet boundary condition: Seek $\Phi \in H^2(\Omega)$ such that

$$\begin{cases} \nabla \cdot (-\mathbf{K}\nabla \Phi) = e_h^\circ, & \mathbf{x} \in \Omega, \\ \Phi = 0, & \mathbf{x} \in \partial\Omega, \end{cases} \tag{47}$$

where $e_h = p_h - Q_h p$. We assume the dual problem has full H^2-regularity and

$$\|\Phi\|_{H^2(\Omega)} \lesssim \|e_h^\circ\|. \tag{48}$$

Theorem 6 (Convergence in pressure) *Assume that $p \in H^{k+1}(\Omega)$, $f \in H^{k-1}(\Omega)$ for $k \geq 1$ or $f \in L^2(\Omega)$ for $k = 0$. Assume the dual problem (47) has H^2-regularity as stated in (48). There holds*

$$\|p - p_h^\circ\| \lesssim h^{k+1}. \tag{49}$$

Proof Testing the 1st equation in (47) with e_h°, we have, by Lemma 2 and the homogeneous boundary condition for Φ in (47),

$$\begin{aligned}
\|e_h^\circ\|^2 &= (\nabla \cdot (-\mathbf{K}\nabla \Phi), e_h^\circ) \\
&= \sum_{E \in \mathcal{E}_h} (\Pi_h(\mathbf{K}\nabla \Phi), \nabla_w e_h)_E
\end{aligned}$$

$$
\begin{aligned}
&= \sum_{E\in\mathcal{E}_h} (\Pi_h(\mathbf{K}\nabla\Phi), \nabla_w(p_h - Q_h p))_E \\
&= \sum_{E\in\mathcal{E}_h} (\Pi_h(\mathbf{K}\nabla\Phi) - \mathbf{K}\nabla\Phi, \nabla_w(p_h - Q_h p))_E \\
&\quad + \sum_{E\in\mathcal{E}_h} (\mathbf{K}\nabla\Phi, \nabla_w(p_h - Q_h p))_E. \qquad (50)
\end{aligned}
$$

By (22) and Lemma 3, the first term on the right-hand side of (50) can be estimated as

$$
\begin{aligned}
&\textstyle\sum_{E\in\mathcal{E}_h} (\Pi_h(\mathbf{K}\nabla\Phi) - \mathbf{K}\nabla\Phi, \nabla_w(p_h - Q_h p))_E \\
&\quad\lesssim \|\nabla\Phi - \Pi_h(\nabla\Phi)\| \, \|\nabla_w(p_h - Q_h p)\| \\
&\quad\lesssim h^{k+1}\|\Phi\|_{H^2(\Omega)} \lesssim h^{k+1}\|e_h^\circ\|. \qquad (51)
\end{aligned}
$$

Next we rewrite the second term on the right-hand side of (50) as follows

$$
\begin{aligned}
&\sum_{E\in\mathcal{E}_h} (\mathbf{K}\nabla\Phi, \nabla_w(p_h - Q_h p))_E \\
&= \sum_{E\in\mathcal{E}_h} (\mathbf{K}\nabla\Phi - \mathbf{Q}_h(\mathbf{K}\nabla\Phi), \nabla_w p_h - \nabla p)_E + \sum_{E\in\mathcal{E}_h} (\mathbf{K}\nabla\Phi - \mathbf{Q}_h(\mathbf{K}\nabla\Phi), \nabla p)_E \\
&\quad + \sum_{E\in\mathcal{E}_h} (\mathbf{Q}_h(\mathbf{K}\nabla\Phi), \nabla_w p_h)_E - \sum_{E\in\mathcal{E}_h} (\mathbf{K}\nabla\Phi, \nabla_w(Q_h p))_E \\
&:= T_1 + T_2 + T_3 + T_4. \qquad (52)
\end{aligned}
$$

Term T_1 can be estimated as (by applying (21), (48), and Corollary 1)

$$
T_1 \lesssim h^{k+1}\|\Phi\|_{H^2(\Omega)} \lesssim h^{k+1}\|e_h^\circ\|. \qquad (53)
$$

Term T_2 can be estimated as (by applying (21) and (48))

$$
\begin{aligned}
T_2 &= \sum_{E\in\mathcal{E}_h} (\mathbf{K}\nabla\Phi - \mathbf{Q}_h(\mathbf{K}\nabla\Phi), \nabla p - \mathbf{Q}_h(\nabla p))_E \\
&\lesssim h^{k+1}\|\Phi\|_{H^2(\Omega)} \lesssim h^{k+1}\|e_h^\circ\|. \qquad (54)
\end{aligned}
$$

For term T_3, we apply Lemma 1 and (8) to obtain

$$
\begin{aligned}
T_3 &= \sum_{E\in\mathcal{E}_h} (\mathbf{K}\mathbf{Q}_h(\nabla\Phi), \nabla_w p_h)_E \\
&= \sum_{E\in\mathcal{E}_h} (\mathbf{K}\nabla_w(Q_h\Phi), \nabla_w p_h)_E \\
&= \sum_{E\in\mathcal{E}_h} (f, Q_h^\circ\Phi)_{E^\circ}. \qquad (55)
\end{aligned}
$$

For term T_4, we apply Lemma 1, (21), (48), the orthogonality implied by $\mathbf{Q}_h$, and the self-adjointness of $\mathbf{K}$. This leads to

$$
\begin{aligned}
T_4 &= -\sum_{E\in\mathcal{E}_h} (\mathbf{K}\nabla\Phi, \mathbf{Q}_h(\nabla p))_E \\
&= \sum_{E\in\mathcal{E}_h} (\mathbf{Q}_h(\mathbf{K}\nabla\Phi) - \mathbf{K}\nabla\Phi, \mathbf{Q}_h(\nabla p) - \nabla p)_E - \sum_{E\in\mathcal{E}_h} (\mathbf{K}\nabla\Phi, \nabla p)_E
\end{aligned}
$$

$$\lesssim h^{k+1}\|e_h^\circ\| - \sum_{E\in\mathcal{E}_h}(f,\Phi)_E. \tag{56}$$

By (55), (56), the approximation properties of Q_h° and Q_h^∂, (48), we have

$$\begin{aligned} T_3+T_4 &\lesssim h^{k+1}\|e_h^\circ\| + \sum_{E\in\mathcal{E}_h}(f-Q_h^\circ f, Q_h^\circ\Phi-\Phi)_E \\ &\lesssim h^{k+1}\|e_h^\circ\| + h^{k-1}h^2\|\Phi\|_{H^2} \\ &\lesssim h^{k+1}\|e_h^\circ\|. \end{aligned} \tag{57}$$

Finally, combining (50), (51), (53), (54), and (57), we obtain

$$\|e_h^\circ\| \lesssim h^{k+1}. \tag{58}$$

The estimate (49) in Theorem 6 follows from (58), the approximation property of Q_h°, and a triangle inequality. □

6 Implementation and Numerical Experiments

For the WG $(P_k, P_k; AC_k)$ finite element methods, the unknowns constitute P_k-type polynomials for element interiors and P_k-type polynomials for edges, but AC_k is not a part of the unknowns. More specifically, to approximate the scalar primal variable, we have two groups of basis functions: degree k polynomials for element interiors and degree k polynomials for edges. The two groups of local basis functions are completely separate. For the interior of each individual quadrilateral, its basis functions can be chosen as monomials

$$1,\quad X,\quad Y,\quad X^2,\quad XY,\quad Y^2,\quad \ldots,$$

where $X = x - x_c$, $Y = y - y_c$ are the normalized coordinates [18] with (x_c, y_c) being the element center. For each edge, we use basis functions $1, s, s^2, \ldots$, where $s \in [-\frac{1}{2}, \frac{1}{2}]$ is the parameter for the line segment.

For the above basis functions, their discrete weak gradients are established in the Arbogast–Correa spaces using formula (6). For the AC_k spaces, we need only their local basis functions on each quadrilateral. Similarly, we use the normalized coordinates.

For $k = 0$, we have $\dim(AC_0) = 4$. A local basis can be chosen as

$$\begin{bmatrix}1\\0\end{bmatrix},\quad \begin{bmatrix}0\\1\end{bmatrix},\quad \begin{bmatrix}X\\Y\end{bmatrix},\quad \mathcal{P}_E\begin{bmatrix}\hat{x}\\-\hat{y}\end{bmatrix},$$

where X, Y are the normalized coordinates as discussed before, $(\hat{x}, \hat{y})$ are the reference coordinates in the reference element $[0, 1]^2$, and $\mathcal{P}_E$ is the Piola transformation (matrix).

For $k = 1$, one has $\dim(AC_1) = 10$. A local basis can be chosen as

$$\begin{bmatrix}1\\0\end{bmatrix},\ \begin{bmatrix}X\\0\end{bmatrix},\ \begin{bmatrix}Y\\0\end{bmatrix},\ \begin{bmatrix}0\\1\end{bmatrix},\ \begin{bmatrix}0\\X\end{bmatrix},\ \begin{bmatrix}0\\Y\end{bmatrix},\ \begin{bmatrix}X^2\\XY\end{bmatrix},\ \begin{bmatrix}XY\\Y^2\end{bmatrix},$$
$$\mathcal{P}_E\begin{bmatrix}1-\hat{x}^2\\2\hat{x}\hat{y}\end{bmatrix},\quad \mathcal{P}_E\begin{bmatrix}2\hat{x}\hat{y}\\1-\hat{y}^2\end{bmatrix},$$

For higher order $AC_k (k \geq 2)$ spaces, their local basis functions can be constructed in a similar way.

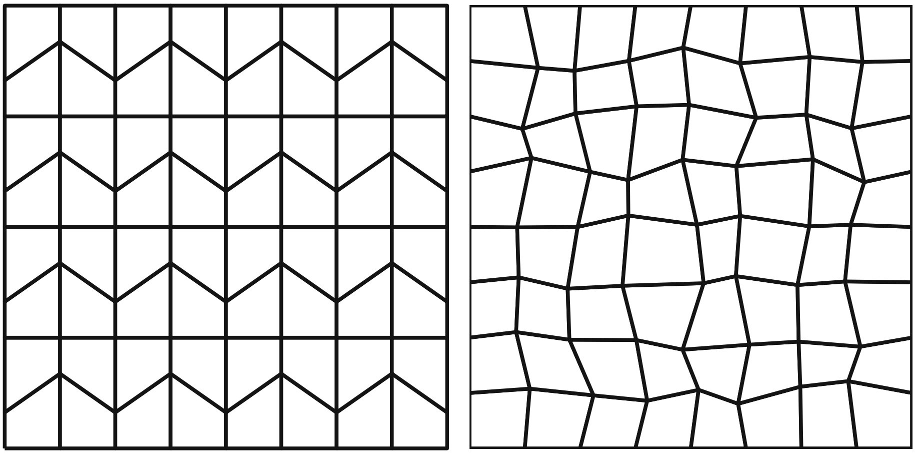

Fig. 1 Quadrilateral meshes used in numerical tests: Left: a trapezoidal mesh used in Example 1 (see [4]); Right: a randomly h-perturbed quadrilateral mesh used in Example 3

Next we present three numerical examples to demonstrate the accuracy of this family of new WG methods. These include tests on a low regularity case and rough quadrilateral meshes, as shown in Fig. 1 right panel.

Example 1 For this example, the domain is $\Omega = (0,1)^2$, the conductivity matrix is $\mathbf{K} = \mathbf{I}_2$ (the order 2 identity matrix). The exact solution is $p(x,y) = \sin(\pi x)\sin(\pi y)$, which is infinitely smooth. So is the right-hand side $f(x,y) = 2\pi^2\sin(\pi x)\sin(\pi y)$. Dirichlet boundary conditions are posed on all four sides.

We consider a sequence of trapezoidal meshes introduced in [4]. They are obtained by modifying the corresponding square meshes. As shown in Fig. 1 left panel, the interior nodes on the vertical lines are moved up or down by αh, where h is the mesh size of the corresponding square mesh and $\alpha = 0.35$ for this example.

As shown in Table 1, when the new methods WG $(P_k, P_k; AC_k)(k = 0, 1, 2)$ are applied to this example, the convergence rates in pressure, velocity, normal flux, and div of velocity are all close to order $k + 1$.

Example 2 (Low regularity) This example is adopted from [28]. One has $\Omega = (0,1)^2$, $p(x,y) = x(1-x)y(1-y)\sqrt{x^2+y^2}^{(\gamma-2)}$ with $\gamma \in (0,1]$ being a regularity parameter. The smoothness of $p(x,y)$ is about $1+\gamma$, since

$$p \in H^{1+\gamma-\varepsilon}(\Omega) \qquad \text{for any small } \varepsilon > 0.$$

We choose $\gamma = 0.4$ for numerical tests. Shown in Table 2 are the results for Example 2 on rectangular meshes obtained from applying the WG $(P_k, P_k; AC_k)$ methods ($k = 0, 1, 2$ respectively). Here are some observations.

(i) For interior pressure approximation, close to first order accuracy is obtained for $k = 0$, since only constant approximants are used. For $k = 1, 2$, higher order polynomial approximants are used, but the accuracy is only about order 1.4, which is the regularity order of the exact solution.

(ii) For approximations to the velocity and normal flux, convergence order is about 0.4, again in agreement with the regularity parameter γ.

Table 1 Example 1: results by $WG(P_k, P_k; AC_k)$ on trapezoidal meshes ($\alpha = 0.35$)

$1/h$	$\|p - p_h^\circ\|$	$\|\mathbf{u} - \mathbf{u}_h\|$	$\|(\mathbf{u} - \mathbf{u}_h) \cdot \mathbf{n}\|_{\mathcal{F}_h}$	$\|\nabla \cdot (\mathbf{u} - \mathbf{u}_h)\|$
WG $(P_0, P_0; AC_0)$				
8	8.3731E−2	2.7626E−1	3.5548E−1	1.6478E−0
16	4.1987E−2	1.3959E−1	1.7236E−1	8.2817E−1
32	2.1009E−2	7.0284E−2	8.4432E−2	4.1462E−1
64	1.0506E−2	3.5272E−2	4.1763E−2	2.0738E−1
Conv.rate	0.998	0.989	1.029	0.996
WG $(P_1, P_1; AC_1)$				
8	8.1312E−3	1.8538E−2	2.3320E−2	1.6046E−1
16	2.0440E−3	4.7109E−3	5.4636E−3	4.0345E−2
32	5.1171E−4	1.1860E−3	1.3361E−3	1.0101E−2
64	1.2797E−4	2.9746E−4	3.3138E−4	2.5260E−3
Conv.rate	1.996	1.987	2.045	1.996
WG $(P_2, P_2; AC_2)$				
8	5.6112e−04	1.7503e−03	3.5197e−03	1.1055e−02
16	7.0430e−05	2.2278e−04	4.5686e−04	1.3895e−03
32	8.8124e−06	2.7985e−05	5.7665e−05	1.7393e−04
64	1.1018e−06	3.5033e−06	7.2252e−06	2.1754e−05
Conv.rate	2.997	2.988	2.976	2.996

Table 2 Example 2: lower regularity captured by $WG(P_k, P_k; AC_k)$ on rectangular meshes

$1/h$	$\|p - p_h^\circ\|$	$\|\mathbf{u} - \mathbf{u}_h\|$	$\|(\mathbf{u} - \mathbf{u}_h) \cdot \mathbf{n}\|_{\mathcal{F}_h}$	$\|\nabla \cdot (\mathbf{u} - \mathbf{u}_h)\|$
WG $(P_0, P_0; AC_0)$				
8	2.4146E−2	4.0407E−1	1.1459E−0	5.9433E+1
16	1.1492E−2	3.0671E−1	8.6487E−1	9.0508E+1
32	5.6244E−3	2.3289E−1	6.5431E−1	1.3751E+2
64	2.7883E−3	1.7678E-1	4.9552E−1	2.0868E+2
Rate	1.038	0.397	0.403	− 0.603
WG $(P_1, P_1; AC_1)$				
8	1.1761E−2	3.5783E−1	9.9503E−1	5.5537E+1
16	4.6056E−3	2.7241E−1	7.5712E−1	8.4649E+1
32	1.7716E−3	2.0695E−1	5.7504E−1	1.2867E+2
64	6.7630E−4	1.5704E−1	4.3629E−1	1.9530E+2
Rate	1.373	0.396	0.396	− 0.604
WG $(P_2, P_2; AC_2)$				
8	6.3140E−3	3.5651E−1	7.1432E−1	4.9062E+1
16	2.4094E−3	2.7117E−1	5.4320E−1	7.4811E+1
32	9.1629E−4	2.0589E−1	4.1239E−1	1.1373E+2
64	3.4785E−4	1.5618E−1	3.1281E−1	1.7265E+2
Rate	1.394	0.396	0.397	− 0.605

Table 3 Example 3: numerical results of $WG(P_1, P_1; AC_1)$ on rectangular and **rough** quadrilateral meshes

$1/h$	$\|p - p_h^\circ\|$	$\|\mathbf{u} - \mathbf{u}_h\|$	$\|(\mathbf{u} - \mathbf{u}_h) \cdot \mathbf{n}\|_{\mathcal{F}_h}$	$\|\nabla \cdot (\mathbf{u} - \mathbf{u}_h)\|$
Uniform rectangular meshes				
8	5.2258E−4	1.1521E-2	1.6859E-2	1.0180E-1
16	1.3166E-4	2.8673E-3	4.0922E−3	2.5449E−2
32	3.2980E−5	7.1601E−4	1.0151E−3	6.3622E−3
64	8.2489E−6	1.7894E−4	2.5324E−4	1.5906E−3
128	2.0625E−6	4.4731E−5	6.3272E−5	3.9764E−4
Conv.rate	1.996	2.002	2.014	2.000
Rough quadrilateral meshes				
8	5.5264E−4	1.4563E−2	2.1653E−2	1.0672E−1
16	1.4409E−4	4.1841E−3	6.0144E−3	2.7205E−2
32	3.6310E−5	1.0103E−3	1.4843E−3	6.8362E−3
64	9.0886E−6	2.5930E−4	3.7590E−4	1.7173E−3
128	2.2727E−6	6.5301E−5	9.4417E−5	4.2845E−4
Conv.rate	1.981	1.950	1.960	1.990

(iii) Divergence of errors in velocity div is observed. This is not a surprise, since the exact solution has low regularity. The error analysis shows that $f \in H^1(\Omega)$ ensures convergence of errors in velocity div. But for this example, we even do not have $f \in L^2(\Omega)$.

Example 3 (Full permeability tensor, rough quadrilateral meshes) This example is adopted from [3] (Example 2 therein). This was considered as a relative hard example, due to the significant tangential fluxes on the element boundaries. Specifically, the domain is $\Omega = (0, 1)^2$, the permeability or conductivity is a full 2×2 matrix

$$\mathbf{K} = \begin{bmatrix} 11 & 9 \\ 9 & 13 \end{bmatrix},$$

whose two positive eigenvalues ($\lambda_1 = 21.0554, \lambda_2 = 2.9446$) are about one magnitude apart. The eigenvector corresponding to λ_1 is $[0.6669, 0.7451]^T$, which is almost parallel to the diagonal direction. This causes a large diagonal component to the flow ([3] Figure 6.1). A known exact solution is given as

$$p(x, y) = x(1-x)y(1-y).$$

Dirichlet boundary conditions are posed on the left and right sides, whereas Neumann conditions are posed on the bottom and top sides.

We test WG $(P_1, P_1; AC_1)$ on both rectangular and rough quadrilateral meshes. The rough meshes are random perturbations of the rectangular meshes, which allow interior nodes to be moved by a magnitude up to $0.25h$. As shown in Table 3, the new WG $(P_1, P_1; AC_1)$ method works well on these rough quadrilateral meshes, although these meshes are not nested.

7 Concluding Remarks

In this paper, we have developed a family of new weak Galerkin finite element methods for elliptic problems on general convex quadrilateral meshes. These new methods are established using the Arbogast–Correa spaces [1].

Our WG methods share some features with the hybridized mixed FEMs, but are developed from a different viewpoint based on reconstruction of a discrete gradient for the primal variable.

(i) Our methods are in the weak Galerkin framework based on the new concepts such as discrete weak gradients.
(ii) WG methods and hybridized mixed FEMs both result in SPD linear systems, via different approaches though.
(iii) In our WG schemes, Dirichlet conditions are essential whereas Neumann conditions are natural. It is the other way around in the mixed methods.
(iv) In terms of implementation, our WG methods need elementwise discrete weak gradients, which involve the local basis functions of AC_k. For the hybridized mixed methods [1], global basis functions are used.
(v) For the mixed methods, local mass conservation and normal flux continuity are obtained through the construction of finite element subspaces. For the WG methods, these properties are obtained through the bilinear forms, as shown in proofs of Theorems 1 and 2.

Compared to the simple WG methods in our previous work [19], the new WG methods in this paper are more sophisticated and apply to general quadrilateral meshes. The WG methods in [19] use the unmapped Raviart–Thomas (RT) spaces for discrete weak gradients. For a quadrilateral, a basis for the unmapped $RT_{[0]}$ space can be chosen as

$$\begin{bmatrix} 1 \\ 0 \end{bmatrix}, \quad \begin{bmatrix} 0 \\ 0 \end{bmatrix}, \quad \begin{bmatrix} X \\ Y \end{bmatrix}, \quad \begin{bmatrix} X \\ -Y \end{bmatrix}.$$

These are all polynomials and hence easy to use. But an “asymptotically parallelogram” condition needs to be assumed for convergence. For the new WG methods in this paper, discrete weak gradients are established in the Arbogast–Correa (AC) spaces, which involve rational functions. For example, in the above basis,

$$\begin{bmatrix} X \\ -Y \end{bmatrix} \quad \text{is replaced by} \quad \mathcal{P}_E \begin{bmatrix} \hat{x} \\ -\hat{y} \end{bmatrix}.$$

This allows quadrilaterals to be general.

Compared to the WG methods in [20,21], our WG methods have some additional nice features.

(i) No penalization is needed for the new WG methods in this paper;
(ii) Full order accuracy in approximation of all four quantities (primal variable, flux, normal flux, and div of flux) are attained.

As previously discussed, HDG is another class of finite element methods that have been devised for all types of PDE problems. Among the existing HDG methods for the second order elliptic problems, the work in [11,13] are noticeable. Both include designs of finite elements for quadrilaterals. A novel approach *M-decomposition* was investigated in [11]. Roughly speaking, the space for multipliers could be decomposed in a way that is related to the normal traces of solenoidal fluxes and the traces of constants in the space for approximating the primal variable. The M-decomposition motivates design of finite elements with super-convergence properties. It will be interesting to see whether the analysis of HDG finite elements on quadrilaterals presented in [11] Table 10 could be borrowed for investigating super-convergence of WG finite elements.

The new WG methods in this paper have been implemented in our `Matlab` code package `DarcyLite`. The methods extend naturally to cuboidal hexahedral meshes when the Arbogast–Tao (AT) spaces [2] are utilized in lieu of the Arbogast–Correa spaces. An interesting question is then how to unify implementations of the AT and AC spaces along with the WG framework. This is currently under our investigation and will be reported in our future work.

Acknowledgements J. Liu and Z. Wang were supported in part by US National Science Foundation under Grant DMS-1819252. S. Tavener was supported in part by US National Science Foundation under Grant DMS-1720473. We sincerely thank the anonymous reviewers for their constructive comments, which have helped improve the quality of this paper.

References

1. Arbogast, T., Correa, M.: Two families of H(div) mixed finite elements on quadrilaterals of minimal dimension. SIAM J. Numer. Anal. **54**, 3332–3356 (2016)
2. Arbogast, T., Tao, Z.: Construction of H(div)-conforming mixed finite elements on cuboidal hexahedra. Numer. Math. **142**, 1–32 (2019)
3. Arbogast, T., Wheeler, M.F., Yotov, I.: Mixed finite elements for elliptic problems with tensor coefficients as cell-centered finite differences. SIAM J. Numer. Anal. **34**, 828–852 (1997)
4. Arnold, D., Boffi, D., Falk, R.: Approximation by quadrilateral finite elements. Math. Comput. **71**, 909–922 (2002)
5. Arnold, D., Boffi, D., Falk, R.: Quadrilateral H(div) finite elements. SIAM J. Numer. Anal. **42**, 2429–2451 (2005)
6. Arnold, D.N., Brezzi, F.: Mixed and nonconforming finite element methods: implementation, postprocessing and error estimates. Math. Model. Numer. Anal. **19**, 7–32 (1985)
7. Brezzi, F., Fortin, M.: Mixed and hybrid finite element methods. Springer, Berlin (1991)
8. Bush, L., Ginting, V.: On the application of the continuous Galerkin finite element method for conservation problems. SIAM J. Sci. Comput. **35**, A2953–A2975 (2013)
9. Chen, W., Wang, F., Wang, Y.: Weak Galerkin method for the coupled Darcy–Stokes flow. IMA J. Numer. Anal. **36**, 897–921 (2016)
10. Cockburn, B.: Static condensation, hybridization, and the devising of the HDG methods. In: Barrenechea, G.R., Brezzi, F. (eds.) Building Bridges: Connection and Challenges in Modern Approaches to Numerical Partial Differential Equations, pp. 129–177. Springer, Berlin (2016)
11. Cockburn, B., Fu, G., Sayas, F.-J.: Superconvergence by M-decompositions. Part I: general theory for HDG methods for diffusion. Math. Comput. **86**, 1609–1641 (2017)
12. Cockburn, B., Gopalakrishnan, J., Lazarov, R.: Unified hybridization of discontinuous galerkin, mixed, and continuous Galerkin methods for second order elliptic problems. SIAM J. Numer. Anal. **47**, 1319–1365 (2009)
13. Cockburn, B., Qiu, W., Shi, K.: Superconvergent HDG methods on isoparametric elements for second-order elliptic problems. SIAM J. Numer. Anal. **50**, 1417–1432 (2012)
14. Ginting, V., Lin, G., Liu, J.: On application of the weak Galerkin finite element method to a two-phase model for subsurface flow. J. Sci. Comput. **66**, 225–239 (2016)
15. Harper, G., Liu, J., Tavener, S., Zheng, B.: Lowest-order weak Galerkin finite element methods for linear elasticity on rectangular and brick meshes. J. Sci. Comput. **78**(3), 1917–1941 (2019)
16. Ingram, R., Wheeler, M.F., Yotov, I.: A multipoint flux mixed finite element method on hexahedra. SIAM J. Numer. Anal. **48**, 1281–1312 (2010)
17. Lin, G., Liu, J., Mu, L., Ye, X.: Weak Galerkin finite element methods for Darcy flow: anistropy and heterogeneity. J. Comput. Phys. **276**, 422–437 (2014)
18. Liu, J., Cali, R.: A note on the approximation properties of the locally divergence-free finite elements. Int. J. Numer. Anal. Model. **5**, 693–703 (2008)

19. Liu, J., Tavener, S., Wang, Z.: The lowest-order weak Galerkin finite element methods for the Darcy equation on quadrilateral and hybrid meshes. J. Comput. Phys. **359**, 312–330 (2018)
20. Mu, L., Wang, J., Ye, X.: Weak Galerkin finite element methdos on polytopal meshes. Int. J. Numer. Anal. Model. **12**, 31–53 (2015)
21. Mu, L., Wang, J., Ye, X.: A weak Galerkin finite element method with polynomial reduction. J. Comput. Appl. Math. **285**, 45–58 (2015)
22. Mu, L., Wang, J., Ye, X., Zhang, S.: A discrete divergence free weak Galerkin finite element method for the Stokes equations. Appl. Numer. Math. **125**, 172–182 (2018)
23. Sun, S., Liu, J.: A locally conservative finite element method based on piecewise constant enrichment of the continuous Galerkin method. SIAM J. Sci. Comput. **31**, 2528–2548 (2009)
24. Wang, C., Wang, J., Wang, R., Zhang, R.: A locking-free weak Galerkin finite element method for elasticity problems in the primal formulation. J. Comput. Appl. Math. **307**, 346–366 (2016)
25. Wang, J., Ye, X.: A weak Galerkin finite element method for second order elliptic problems. J. Comput. Appl. Math. **241**, 103–115 (2013)
26. Wang, J., Ye, X.: A weak Galerkin mixed finite element method for second order elliptic problems. Math. Comput. **83**, 2101–2126 (2014)
27. Wheeler, M., Xue, G., Yotov, I.: A multipoint flux mixed finite element method on distorted quadrilaterals and hexahedra. Numer. Math. **121**, 165–204 (2012)
28. Wihler, T., Riviére, B.: Discontinuous Galerkin methods for second-order elliptic PDE with low-regularity solutions. J. Sci. Comput. **46**, 151–165 (2011)
29. Yi, S.-Y.: A lowest-order weak Galerkin method for linear elasticity. J. Comput. Appl. Math. **350**, 286–298 (2019)